



Contents lists available at ScienceDirect

# Colloids and Surfaces A: Physicochemical and Engineering Aspects

journal homepage: [www.elsevier.com/locate/colsurfa](http://www.elsevier.com/locate/colsurfa)

## Collective motion of catalytic particles driven by abiotic aerobic metabolism

Daigo Yamamoto<sup>a,\*</sup>, Tsuyoshi Takada<sup>a</sup>, Yuto Io<sup>a</sup>, Masaki Kubouchi<sup>a</sup>, Yasunao Okamoto<sup>b</sup>, Erika Okita<sup>c</sup>, Kenichi Yoshikawa<sup>d</sup>, Akihisa Shioi<sup>a</sup>

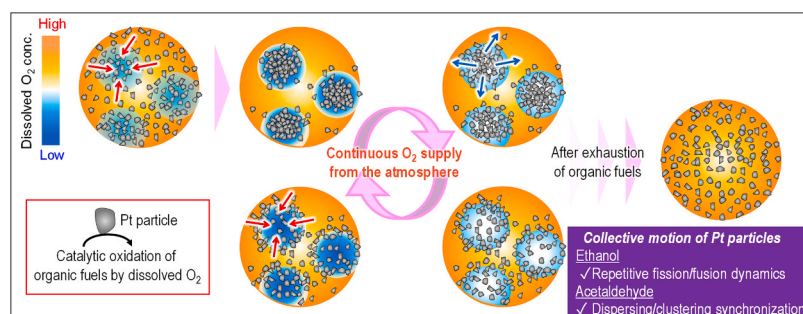
<sup>a</sup> Department of Chemical Engineering and Materials Science, Doshisha University, Kyoto 610-0321, Japan

<sup>b</sup> Research Center for Membrane and Film Technology, Kobe University, Kobe 657-8501, Japan

<sup>c</sup> Department of Chemical Engineering, Osaka Metropolitan University, Osaka 599-8531, Japan

<sup>d</sup> Faculty of Life and Medical Sciences, Doshisha University, Kyoto 610-0394, Japan

### GRAPHICAL ABSTRACT



### ARTICLE INFO

#### Keywords:

Self-organization  
Collective motion  
Synchronization  
Catalytic particles  
Organic fuel

### ABSTRACT

The phenomenon of collective motion of Pt particles (primary particles and aggregates) immersed in water containing organic fuels has been observed. Over time, these Pt particles tend to aggregate into numerous schools at the bottom of the container. Subsequently, unique spatiotemporal patterns emerge, including repetitive fission/fusion dynamics and dispersing/clustering synchronization among schools. Notably, the species of organic fuels influence the observed patterns. Pt particles exhibit self-propulsion through catalytic oxidation of organic fuels by dissolved oxygen, mirroring the chemical mechanism seen in living organisms. This contrast with previous studies on chemically propelled objects underscores the biomimetic nature of the system, highlighting its resemblance to living processes. This self-propelled system, operating with an aerobic metabolic mechanism, presents a valuable real-world model for elucidating the fundamental principles underlying collective motion in living organisms.

\* Corresponding author.

E-mail address: [dyamamot@mail.doshisha.ac.jp](mailto:dyamamot@mail.doshisha.ac.jp) (D. Yamamoto).

<https://doi.org/10.1016/j.colsurfa.2024.134580>

Received 10 May 2024; Received in revised form 8 June 2024; Accepted 20 June 2024

Available online 24 June 2024

0927-7757/© 2024 The Author(s). Published by Elsevier B.V. This is an open access article under the CC BY license (<http://creativecommons.org/licenses/by/4.0/>).

## 1. Introduction

Self-organization consists of various space–time structures formed by multiple components. The structure-forming process is interesting and applicable to bio- and microtechnologies. These structures are classified into static or dynamic self-organization [1]. Static self-organization manifests in colloidal crystal [2,3], Langmuir–Blodgett film [4,5], and supramolecular assemblies [6,7]. These structures evolve under thermodynamically stable conditions, progressing towards equilibrium following their kinetics toward equilibrium. In contrast, dynamic self-organization occurs in open systems far from thermal equilibrium [8]. Many research groups have explored artificial dynamic self-organizations, yielding various spatiotemporal patterns across scales, including reaction-diffusion waves [9,10], collective motions of active matters [11,12], and self-assembled particles under external dynamic fields [13,14]. Collective motion, or swarming behavior, is a focal point of research due to its unique dynamic behavior of living systems [15], evident in phenomena like schools of fish [16,17] and flocks of birds [18]. Even unicellular microorganisms, such as bacteria exhibit geometric patterns, known as colonies, suggesting a simpler mechanism underlying the behavior. The mathematical model proposed by Vicsek et al. [19] has accelerated theoretical studies on the collective motion of active matter, facilitating a deeper understanding of its physical universality [20]. However, the previous models overlooked any concrete chemical or physicochemical processes, such as chemical reactions in the real world.

Over the past two decades, various catalytic microparticles driven by chemical reactions have been studied [21,22]. These active matters mimic biomimetic functions and hold promise in biochemical systems. In particular, catalytic microparticles propelled by the oxidation of organic fuels by dissolved oxygen (aerobic metabolism) serve as a simple real-world model of aquatic microorganisms. Unlike conventional chemical fuels such as hydrogen peroxide and hydrazine, which pose environmental risks, organic materials such as alcohol and aldehydes fuel these microparticles, making them more environmentally friendly [21].

While several research groups have demonstrated the abiotic collective motions of catalytic particles driven by chemical reactions, most prior demonstrations relied on toxic fuels like hydrogen peroxide and/or external stimuli such as UV light [15,23–26]. Here, we demonstrate the collective motions driven by the aerobic metabolism. In this study, we demonstrate collective motion driven by aerobic metabolism.

Our experimental procedure disperses commercial Pt powder in water containing organic fuels and dissolved oxygen. Given that Pt particles exist both as primary particles and aggregates (see Fig. S1 in the Supporting information), their morphologies and consequent motilities were different from each other. We have previously reported that Pt particles exhibit diverse motion, including active Brownian motion, translation, rotation, and spin at the bottom of containers depending on their morphologies [27]. Propulsion arises from the Pt-catalyzed oxidation of organic fuels by dissolved oxygen, mirroring the chemical reactions driving aerobic organisms. The Pt particles convert chemicals into mechanical energy isothermally, with motility decreases at lower oxygen concentrations. Exploring the behavior of biomimetic particles in crowded states presents an intriguing avenue for research, offering fundamental knowledge not only for microtechnologies but also for further revealing the underlying physics of collective motions of living organisms.

## 2. Experimental method

### 2.1. Chemicals

Pt powder (PT-354015, 1  $\mu\text{m}$  in size (Fig. S2 in the Supporting information), 99.95 % purity) was procured from Nilaco Corp. Ethanol (99.5 % purity), acetaldehyde (90 % purity), and hydrogen peroxide

(30 % purity) were purchased from Wako Pure Chemical Industries.

### 2.2. Observation of collective motions of Pt particles

The experimental setup closely resembled prior reports, with variations in the number density of the Pt particles [27]. Initially, Pt particles were dispersed in deionized water by ultrasonication. Subsequently, the particle suspension was then mixed with organic solutes (ethanol or acetaldehyde) to yield a 300 mg/L Pt suspension containing 2 vol% organic solutes. Notably, the number density of the Pt particles was approximately 100 times higher than in our previous study [27], where Pt particles never exhibit the collective motion because of the low number density. The resulting solution (2.0 mL) was poured into a glass-based dish (3910-035, IWAKI), and the collective motion of the Pt particles was observed both macroscopically at room temperature (20–25 °C) using a digital single-lens reflex camera (EOS Kiss X9, Canon) and microscopically using an optical microscope (Olympus IX71, Olympus). As a control, we observed the motion of Pt particles in pure water and water containing hydrogen peroxide (1 wt%).

### 2.3. Measurement of the reaction rate of oxidation with dissolved oxygen in organic fuels

40 mL of a 300 mg/L Pt suspension containing 2 vol% organic solutes was poured into a 50 mL screw bottle (9-852-09, AS ONE Corp.) with stirred vigorously by using a stirrer (RSH-1DN, AS ONE Corp.) and a rotor. The dissolved oxygen meter (HI98193, Hanna Instrument) was inserted into the suspension. Then, the gap between the screw bottle and the dissolved oxygen meter was covered with paraffin film to hinder the oxygen supply from the atmosphere. The series of the above mentioned experimental procedure were performed as rapidly as possible. Time course of the dissolved oxygen concentration was measured.

## 3. Results and discussion

### 3.1. Collective motions of Pt particles

Fig. 1 depicts a typical example of the collective motion of Pt particles in ethanol-containing water at the bottom of a glass dish. The macroscopic pattern post-addition of the Pt particle suspension is shown in Fig. 1a. The Pt particles exist both as primary particles with 1  $\mu\text{m}$  and aggregates (secondary particles) with several micrometers in size (see Fig. S1). Hereinafter the both of them is collectively called "particles". Although the Pt particles were well dispersed and indistinguishable individually, within 20 min, they gradually formed numerous schools across the bottom. Microscopic observations were performed to examine each school in detail (Fig. 1b). Initially, at 0 min, Pt particles were dispersed individually, with numerous minute dark spots representing individual particles, although not clearly visible because of their small size (see Video S1 in the Supporting information). The shapes of dark spots are asymmetric and different from each other, demonstrating that the primary particles and aggregates with various morphologies coexist. Over time, these particles gradually gathered to form schools several tens of micrometers in size. Fig. 1b (blue and red dotted lines) illustrates the fission (64–69 min) and fusion (105–106 min) of each school with translational motion (green arrows at 10 min) and eventual collapse. Such dynamics of fission/fusion bear reminiscent of the collective locomotion observed widely in animals [28]. After a few hours, accompanied by an oxidative reaction consuming ethanol, the particles within schools tended to disperse. This redispersion was attributed to the effect of Brownian motion (420 min) (see Video S1 for confirmation of the series of collective motions in the Supporting information).

When utilizing acetaldehyde as the organic fuel, distinct spatiotemporal patterns emerge in the collective motion dynamics. Fig. 2a depicts snapshots of this experiment, revealing the formation of the particle schools. Unlike the ethanol system, where the particles displayed

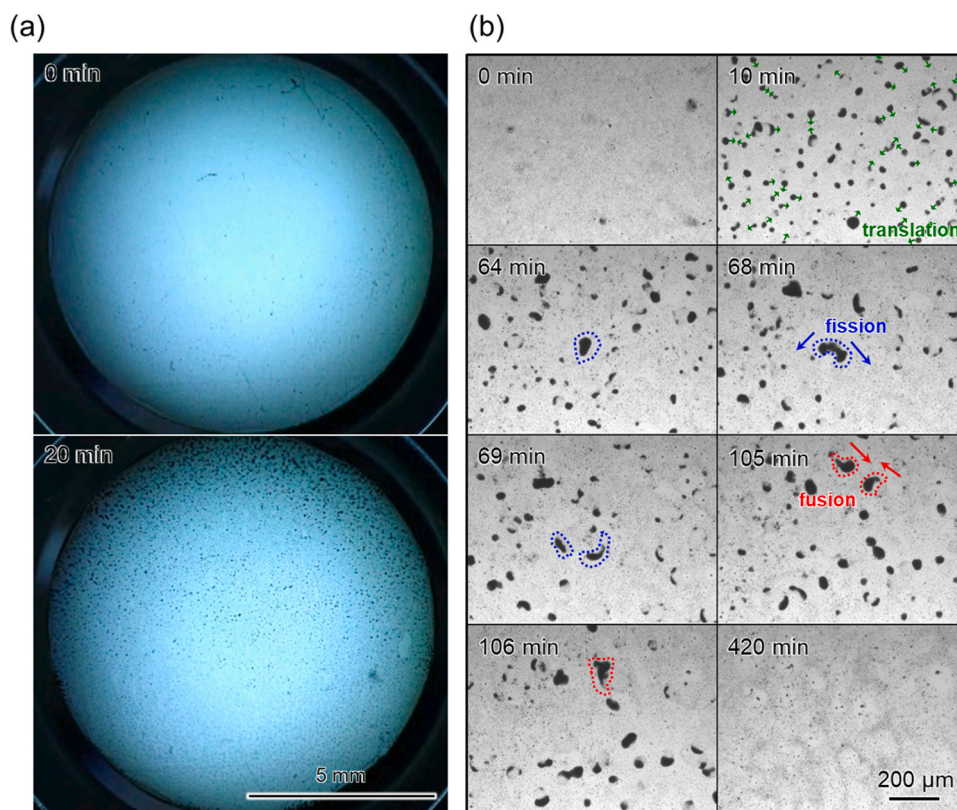


**Fig. 1.** Collective motion of Pt particles was observed in 2.0 vol% ethanol–water on the bottom of the glass dish. The motion was captured using (a) a digital single-lens reflex camera and (b) an optical microscope at room temperature. The recorded time indicates the duration after the settling of convection induced by pouring the Pt suspension that elapsed after the convection settled.

periodic dynamics including clustering and dispersion along with translation, those in the acetaldehyde system exhibited a unique behavior. Notably, over 50 schools observed under the microscope demonstrated synchronized cycles, exhibiting consistent periodicity ranging from 10.4 to 12.7 min (see **Video S2** in the Supporting information). **Fig. 2b** illustrates the temporal evolution of the ratio of school areas in each snapshot from **Video S2** (corresponding to **Fig. 2a**). The total projected area of the schools was quantified through binarization using image analysis software (ImageJ). A similar analysis was applied to the results obtained with ethanol (**Fig. 2c**) (from **Video S1**; corresponding to **Fig. 1b**). We confirmed that the fundamental pattern of the graph remained consistent irrespective of the binarization threshold. The total area of the schools in the acetaldehyde system exhibited oscillations between nearly zero and beyond 0.5, contrasting with the noisy fluctuations of the ethanol system that did not approach zero (**Fig. 2b, c**). Furthermore, the duration of collective motion induced by acetaldehyde was approximately 30 min, shorter than that of ethanol (~ 400 min). This synchronization observed in chemically driven oscillators may serve as a model for various biological phenomena such as neural signaling, heartbeat, and firefly flashing [29].

In our previous study, Pt particles with a low number density exhibited non-Brownian motions, including active Brownian motion and regulated motions when suspended in hydrogen-peroxide-containing water, similar to those in ethanol-containing water [30]. In this study we observed the behavior of Pt particles under approximately 100 times higher number density than those in our previous study in hydrogen peroxide-containing water or pure water as controls. However, the particles in both liquids did not exhibit any collective motion and retained their initial dispersive states (see **Fig. S2** in the **Supporting information**).

Supplementary material related to this article can be found online at [doi:10.1016/j.colsurfa.2024.134580](https://doi.org/10.1016/j.colsurfa.2024.134580).

### 3.2. Collective motion mechanism of Pt particles

In a previous study, we found that Pt particles (aggregates), when in ethanol and hydrogen peroxide fuels, exhibit movement or spin in opposite directions [25]. The oxidations catalyzed by the Pt particles with the aforementioned fuels are described as follows:



To elucidate the difference in movement directions between ethanol and hydrogen peroxide fuels, we postulated that the propulsion arises from an oxygen concentration gradient formed by the shape of the Pt aggregate configuration. The movement of the Pt particles is believed to be driven by this gradient through chemotaxis. Previous studies have reported that the Pt particles descend along a gradient through negative chemotaxis [27]. Based on this hypothesis, we discuss the formation of schools, as illustrated in **Fig. 3**. Achieving perfect dispersion would result in the Pt particles being homogeneously dispersed. However, the observed concentration fluctuation arises from external disturbance, e. g., incomplete mechanical mixing during the actual experiment. In localized regions where the number density of Pt particles exceeds that of the surroundings, the reaction rate is comparatively high, leading to a lower concentration of dissolved oxygen (Eq. (1)). Consequently, a negative gradient of oxygen concentration develops toward this region. The Pt particles in the vicinity to this zone tend to aggregate because of negative chemotaxis (see the red arrows in **Fig. 3a**). As more Pt particles aggregate, the oxygen concentration gradient intensifies. This positive feedback led to rapid and transitional growth in schools. This hypothesis also elucidates why the Pt particles do not exhibit collective motion in hydrogen-peroxide-containing water. The decomposition of hydrogen



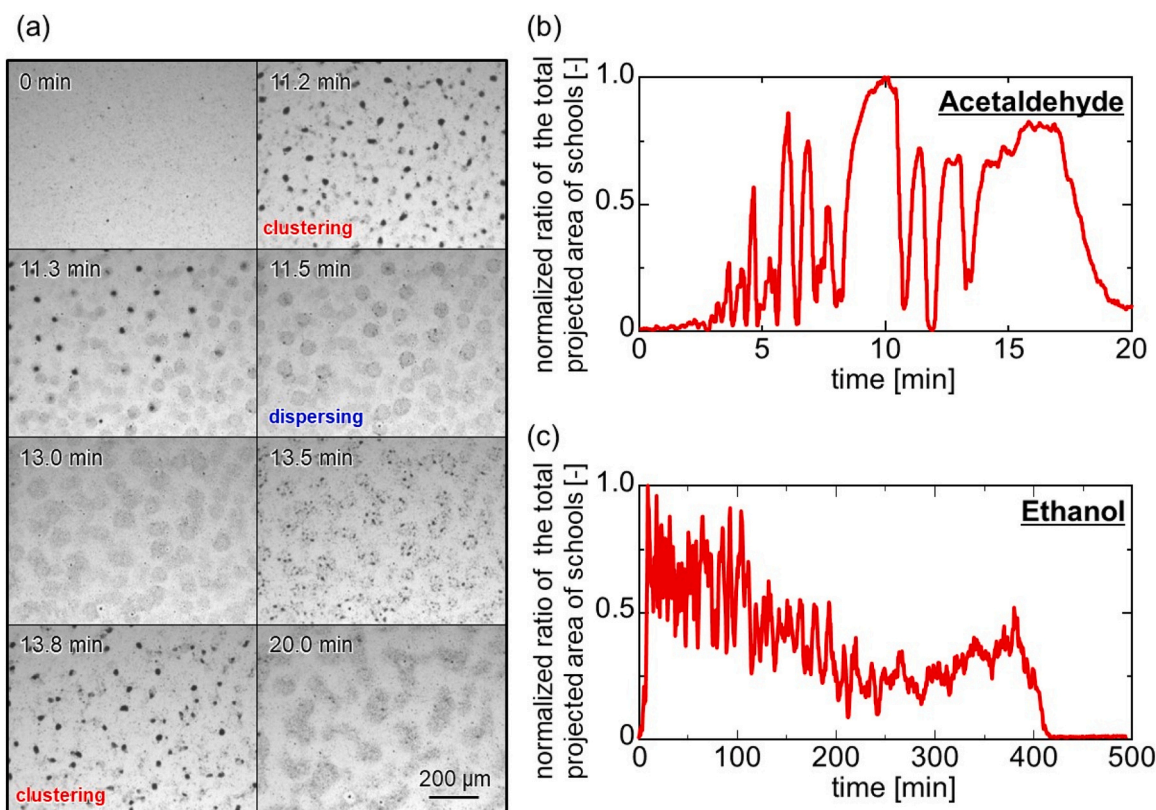


**Fig. 2.** Collapse/clustering synchronization of Pt schools was observed in 2.0 vol% acetaldehyde–water (Video S2 in the Supporting information). (a) Time-lapse optical microscopic images and (b) the time course of the ratio of the total projection area of schools are shown. The total projection area is normalized by the maximum value. The numbers (i)–(vii) correspond to those of (a). (c) Results for the ethanol case corresponds to Fig. 1b and Video S1 in the Supporting information.

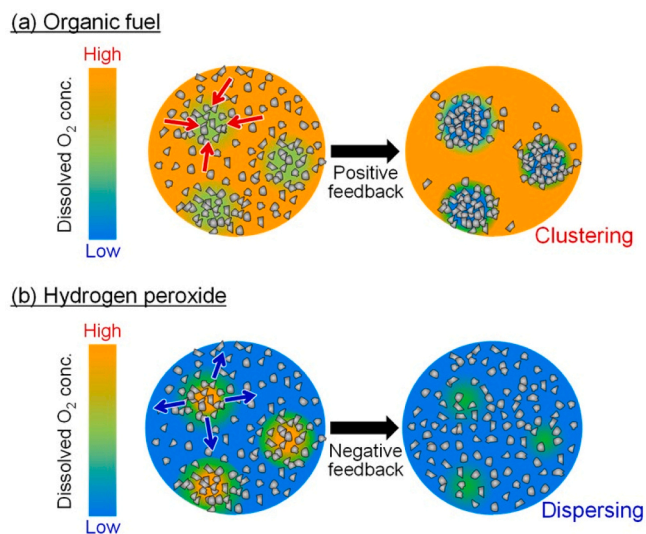


**Fig. 3.** School formation of Pt particles induced by oxidation with dissolved oxygen in (a) organic fuel and (b) hydrogen peroxide.

peroxide (Eq. (2)) elevates the oxygen concentration in regions enriched with the Pt particles (higher reaction rate). As a result, an oxygen concentration gradient opposite to that observed in ethanol (Eq. (1), oxygen-consuming reaction) is generated. This opposite gradient promotes the dispersion of the Pt particles (blue arrows in Fig. 3b).

In our experimental setup, we regulated the concentration of dissolved oxygen concentration by continuously supplying it through mass transfer at the gas–liquid interface. To examine the influence of oxygen

supply on collective motion dynamics, we disrupted the continuous oxygen supply by covering it with a glass dish. In this experiment, we observed a single cycle of collective motion demonstrating clustering and dispersion, which occurred without repetition (Fig. 4; see Video S3 in the Supporting information). Throughout the collective motion, the sizes of the schools increased monotonically, leading to the formation of larger schools (120–240 min in Fig. 4a) through their fusion (32–61 min in Fig. 4b). This result demonstrates that the unique collective dynamics emerge from the highly non-equilibrium nature inherent in the reaction process, where oxygen is supplied continuously.

Supplementary material related to this article can be found online at [doi:10.1016/j.colsurfa.2024.134580](https://doi.org/10.1016/j.colsurfa.2024.134580).

To elucidate the monotonous clustering and subsequent dispersion of Pt particles in the closed system (Fig. 4), we devised the following simple model. The 1-dimensional collective motion model can be described as follows: The flux ( $J_{Pt}$ ) and mass balance of Pt particles at time  $t$  are expressed as

$$J_{Pt} = -D_{Pt} \frac{\partial n_{Pt}}{\partial x} + f \left( -\frac{\partial C_{O_2}}{\partial x} \right) \cdot n_{Pt} - g(n_{Pt}) \cdot n_{Pt} \quad (3)$$

$$\frac{\partial n_{Pt}}{\partial t} = -\frac{\partial J_{Pt}}{\partial x} \quad (4)$$

The first term  $-D_{Pt} \frac{\partial n_{Pt}}{\partial x}$  on the right-hand side represents diffusion by Brownian motion, where  $n_{Pt}$  and  $D_{Pt}$  denote the number density and diffusion coefficient of Pt particles, respectively. The second term  $f \left( -\frac{\partial C_{O_2}}{\partial x} \right) \cdot n_{Pt}$  represents chemotaxis by the oxygen concentration, where,  $C_{O_2}$  denote the dissolved oxygen concentration. Here,  $f$  is a function of the oxygen concentration gradient, serving as the driving force for the Pt particles to actively move towards lower oxygen concentrations. The third term acts as an inhibitor for the positive feedback

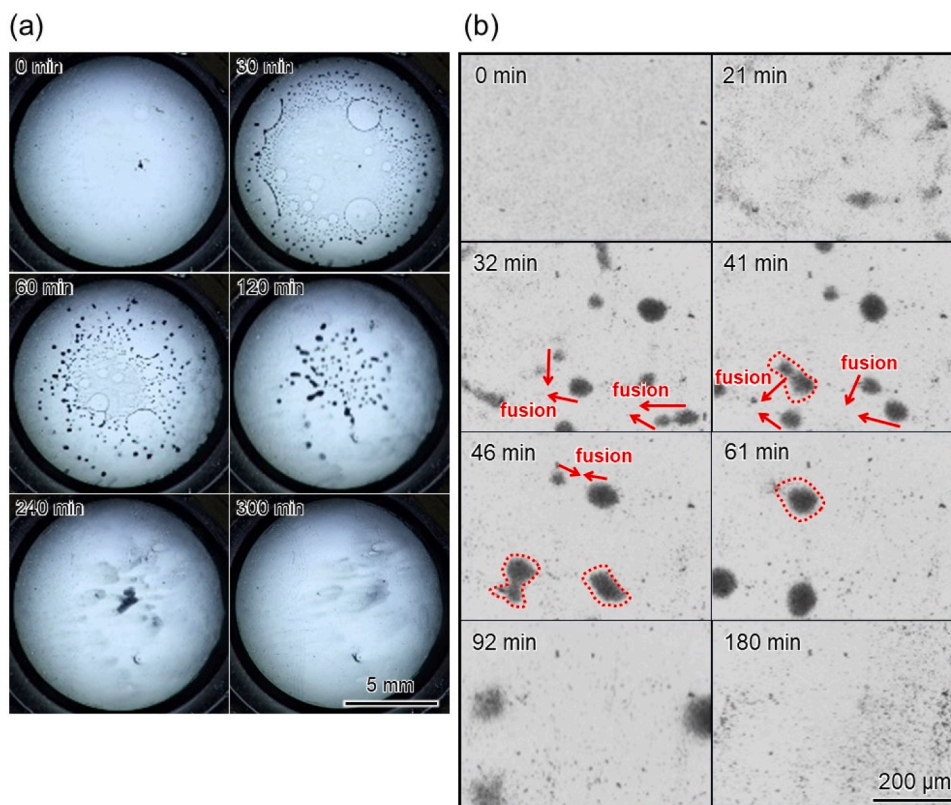


**Fig. 4.** Monotonous clustering and the subsequent dispersing of Pt particles in ethanol–water in the closed system where the oxygen supply from the atmosphere is hindered by covering with a glass dish. The motion was captured using (a) a digital single-lens reflex camera and (b) an optical microscope at room temperature.

(autocatalytic) growth of Pt clusters, preventing infinite growth of  $n_{Pt}$  by reaching the closest packing limit of the particles. The mass conservation of dissolved oxygen and organic fuel X can be expressed as follows:

$$\frac{\partial C_{O_2}}{\partial t} = D_{O_2} \frac{\partial^2 C_{O_2}}{\partial x^2} - r(n_{Pt}, C_{O_2}, C_X) \quad (5)$$

$$\frac{\partial C_X}{\partial t} = D_X \frac{\partial^2 C_X}{\partial x^2} - 2r(n_{Pt}, C_{O_2}, C_X) \quad (6)$$

The first term on the right-hand side represents diffusion by Brownian motion while the second term represents the reaction rate of oxygen (5) and the fuel component (6) catalyzed by the Pt particles. The reaction rate  $r$  is a function of  $n_{Pt}$ ,  $C_{O_2}$ , and  $C_X$ . The partial differential equations (Eqs. (3)–(6)) may explain the unique features of collective motions. Our model, elucidating the monotonous clustering and subsequent dispersion of Pt particles in ethanol–water mixtures, as shown in Fig. 4, can be reproduced (see Note S1, Fig. S3, and Table S1 in the Supporting information).

Although the detailed mechanism that ethanol and acetaldehyde lead to the different modes of the collective motion is unclear at present, the modes may depend on the kinetics of the oxidation reaction. Actually, we measured the consumption rate of the oxidation for ethanol and acetaldehyde in a batch reactor without oxygen supply, we found that the decrease rate of the dissolved oxygen in ethanol is faster than that in acetaldehyde (Fig. 5). Further investigation on the effects of concentrations of both organic fuels and the number density of the Pt particles on the collective motion is required.

#### 4. Conclusions

In this study, we observed unique collective motions within a simple abiotic system, involving commercial Pt particles suspended in water containing organic fuels. We found that the Pt particles exhibit schooling

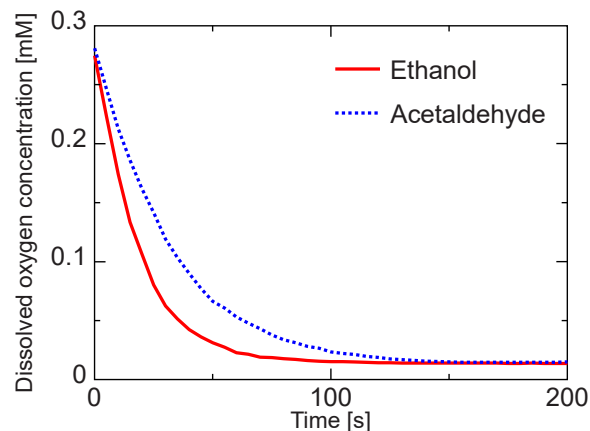


**Fig. 5.** Time course of dissolved oxygen concentration in a 300 mg/L Pt suspension containing 2 vol% organic solutes in the closed system where the oxygen supply is prevented by covering with paraffin film.

behavior characterized by repetitive fission/fusion dynamics and synchronized transitions between dispersive and clustering states. Importantly, the specific type of motion depends on the species of organic fuels. These collective motions of the Pt particles never occur in hydrogen peroxide or pure water, indicating that they arise from the oxidation of the organic fuels by dissolved oxygen. This suggests the similarity in overall chemistry to those of various aquatic organisms. The biomimetic nature of this system, with resembling aerobic metabolism, offers a valuable model for understanding the physics of collective motion. Such a model holds promise for enhancing our understanding of collective behavior in biological and synthetic systems alike.

## CRedit authorship contribution statement

**Akihisa Shioi:** Writing – review & editing, Project administration, Funding acquisition, Conceptualization. **Daigo Yamamoto:** Writing – original draft, Supervision, Project administration, Funding acquisition, Conceptualization. **Yuto Io:** Writing – review & editing, Methodology, Investigation, Formal analysis, Data curation. **Tsuyoshi Takada:** Writing – review & editing, Methodology, Investigation, Formal analysis, Data curation, Conceptualization. **Yasunao Okamoto:** Writing – review & editing, Validation, Resources, Methodology. **Masaki Kubouchi:** Writing – review & editing, Methodology, Investigation, Formal analysis, Data curation. **Kenichi Yoshikawa:** Writing – review & editing, Funding acquisition, Conceptualization. **Erika Okita:** Writing – review & editing, Visualization, Resources, Methodology.

## Declaration of Competing Interest

The authors declare the following financial interests/personal relationships which may be considered as potential competing interests: Daigo Yamamoto reports financial support was provided by Japan Society for the Promotion of Science. Kenichi Yoshikawa reports financial support was provided by Japan Society for the Promotion of Science. Akihisa Shioi reports financial support was provided by Japan Society for the Promotion of Science. If there are other authors, they declare that they have no known competing financial interests or personal relationships that could have appeared to influence the work reported in this paper.

## Data availability

No data was used for the research described in the article.

## Acknowledgements

This work was financially supported by JSPS KAKENHI Grant nos. 20H01878, 22K03560, 20H01877, and 24K08143.

## Declaration of Competing Interest

The authors declare that they have no competing interest.

## Appendix A. Supporting information

Supplementary data associated with this article can be found in the online version at [doi:10.1016/j.colsurfa.2024.134580](https://doi.org/10.1016/j.colsurfa.2024.134580).

## References

- [1] G.M. Whitesides, B. Grzybowski, Self-assembly at all scales, *Science* 295 (2002) 2418–2421.
- [2] F.X. Redl, K.S. Cho, C.B. Murray, S. O'Brien, Three-dimensional binary superlattices of magnetic nanocrystals and semiconductor quantum dots, *Nature* 423 (2003) 968–971.

- [3] F. Li, D.P. Josephson, A. Stein, Colloidal assembly: the road from particles to colloidal molecules and crystals, *Angew. Chem. Int. Ed.* 50 (2011) 360–388.
- [4] J.A. Zasadzinski, R. Viswanathan, L. Madsen, J. Garnæs, D.K. Schwartz, Langmuir-Blodgett films, *Science* 263 (1994) 1726–1733.
- [5] G. Decher, Fuzzy nanoassemblies: toward layered polymeric multicomposites, *Science* 277 (1997) 1232–1237.
- [6] J.M. Lehn, Perspectives in supramolecular chemistry – from molecular recognition towards molecular information processing and self-organization, *Angew. Chem. Int. Ed.* 29 (1990) 1304–1319.
- [7] B. Moulton, M.J. Zaworotko, From molecules to crystal engineering: supramolecular isomerism and polymorphism in network solids, *Chem. Rev.* 101 (2001) 1629–1658.
- [8] M. Fialkowski, K.J.M. Bishop, R. Klajn, S.K. Smoukov, C.J. Campbell, B. A. Grzybowski, Principles and implementations of dissipative (dynamic) self-assembly, *J. Phys. Chem. B* 110 (2006) 2482–2496.
- [9] V. Petrov, Q. Ouyang, H.L. Swinney, Resonant pattern formation in a chemical system, *Nature* 388 (1997) 655–657.
- [10] I. Berenstein, C. Beta, Spatiotemporal chaos arising from standing waves in a reaction-diffusion system with cross-diffusion, *J. Chem. Phys.* 136 (2012) 034903.
- [11] S. Soh, K.J.M. Bishop, B.A. Grzybowski, Dynamic self-assembly in ensembles of camphor boats, *J. Phys. Chem. B* 112 (2008) 10848–10853.
- [12] S. Soh, M. Branicki, B.A. Grzybowski, Swarming in shallow waters, *J. Phys. Chem. Lett.* 2 (2011) 770–774.
- [13] B.A. Grzybowski, H.A. Stone, G.M. Whitesides, Dynamic self-assembly of magnetized, millimetre-sized objects rotating at a liquid-air interface, *Nature* 405 (2000) 1033–1036.
- [14] H. Li, J.R. Friend, L.Y. Yeo, Microfluidic colloidal island formation and erasure induced by surface acoustic wave radiation, *Phys. Rev. Lett.* 101 (2008) 084502.
- [15] Z. Lin, C. Gao, M. Chen, X. Lin, Q. He, Collective motion and dynamic self-assembly of colloid motors, *Curr. Opin. Colloid Interface Sci.* 35 (2018) 51–58.
- [16] A. Huth, C. Wissel, The simulation of the movement of fish schools, *J. Theor. Biol.* 156 (1992) 365–385.
- [17] J.K. Parrish, S.V. Viscido, D. Grünbaum, Self-organized fish schools: an examination of emergent properties, *Biol. Bull.* 202 (2002) 296–305.
- [18] C.K. Hemelrijk, H. Hildenbrandt, Some causes of the variable shape of flocks of birds, *PLoS One* 6 (2011).
- [19] T. Vicsek, A. Czirók, E. Ben-Jacob, I. Cohen, O. Shochet, Novel type of phase transition in a system of self-driven particles, *Phys. Rev. Lett.* 75 (1995) 1226–1229.
- [20] F. Ginelli, The physics of the Vicsek model, *Eur. Phys. J.: Spec. Top.* 225 (2016) 2099–2117.
- [21] D. Yamamoto, A. Shioi, Self-propelled nano/micromotors with a chemical reaction: underlying physics and strategies of motion control, *KONA Powder Part. J.* 32 (2015) 2–22.
- [22] B. Jurado-Sánchez, J. Wang, Micromotors for environmental applications: a review, *Environ. Sci. Nano* 5 (2018) 1530–1544.
- [23] D. Kagan, S. Balasubramanian, J. Wang, Chemically triggered swarming of gold microparticles, *Angew. Chem. Int. Ed.* 50 (2011) 503–506.
- [24] W. Duan, R. Liu, A. Sen, Transition between collective behaviors of micromotors in response to different stimuli, *J. Am. Chem. Soc.* 135 (2013) 1280–1283.
- [25] W. Gao, A. Pei, R. Dong, J. Wang, Catalytic iridium-based janus micromotors powered by ultralow levels of chemical fuels, *J. Am. Chem. Soc.* 136 (2014) 2276–2279.
- [26] T. Si, Z. Wu, W. He, Q. He, Self-propelled predator-prey of swarming Janus micromotors, *iScience* 26 (2023) 106112.
- [27] D. Yamamoto, T. Takada, M. Tachibana, Y. Iijima, A. Shioi, K. Yoshikawa, Micromotors working in water through artificial aerobic metabolism, *Nanoscale* 7 (2015) 13186.
- [28] M.J. Silk, D.P. Croft, T. Tregenza, S. Bearhop, The importance of fission-fusion social group dynamics in birds, *Ibis* 156 (2014) 701–715.
- [29] S.H. Strogatz, *Sync: The Emerging Science of Spontaneous Order*, Hyperion, New York, 2003.
- [30] D. Yamamoto, A. Mukai, N. Okita, K. Yoshikawa, A. Shioi, Catalytic micromotor generating self-propelled regular motion through random fluctuation, *J. Chem. Phys.* 139 (2013) 034705.